ELSEVIER

Journal of Hazardous Materials A67 (1999) 111–144

Journal of Hazardous Materials

Risk-informed selection of a highway trajectory in the neighborhood of an oil-refinery

Ioannis A. Papazoglou [a,*], Zoe Nivolianitou [a], Olga Aneziris [a], Michalis D. Christou [b], Gerasimos Bonanos [a]

[a] *Laboratory of System Reliability and Industrial Safety (LSRIS), Institute of Nuclear Technology-Radiation Protection, National Center for Scientific Research 'Demokritos', Aghia Paraskevi 15310, Greece*
[b] *EC-JRC ISPRA, ISIS, Industrial Hazards Unit, 21020 Ispra, VA, Italy*

Received 1 March 1999; accepted 2 March 1999

Abstract

A methodology for characterizing alternative trajectories of a new highway in the neighborhood of an oil-refinery with respect to the risk to public health is presented. The approach is based on a quantitative assessment of the risk that the storage facilities of flammable materials of the refinery pose to the users of the highway. Physical phenomena with a potential for detrimental consequences to public health such as BLEVE (Boiling Liquid Expanding Vapor Explosion), Unconfined Vapor Cloud Explosion, flash fire and pool fire are considered. Methodological and procedural steps for assessing the individual risk around the tank farm of the oil-refinery are presented. Based on the individual risk, group risk for each alternative highway trajectory is determined.

Keywords: Boiling Liquid Expanding Vapor Explosion; Unconfined Vapor Cloud Explosion; Flash fire; Pool fire; Quantified risk assessment; Oil-refinery; Risk-informed decision making

1. Introduction

This paper presents the methodological and procedural steps for the quantitative risk assessment of a facility storing flammable materials and their application to a tank farm of an oil refinery. Of particular interest is the risk to the users of a highway passing

* Corresponding author. Tel.: +30-1-654-8415; fax: +30-1-654-0926; e-mail: yannisp@ipta.demokritos.gr

0304-3894/99/$ - see front matter
PII: S0304-3894(99)00040-0

close to the refinery. Alternative trajectories of the proposed highway are considered and compared with respect to the risk imposed to its users.

The facility under analysis was established initially at the seashore south of an existing highway (see Fig. 1). Over the years, the storage facilities of the oil-refinery have expanded north of the initial installation and of the existing highway. As a result the facility has ended up as shown in Fig. 1 with the highway passing through the middle. This situation has been qualitatively judged as 'risky' and when a new and wider highway was being planned it was decided to 'bypass' the refinery. Owing to the mountainous terrain north of the refinery the economic cost of constructing the new highway was significantly increasing with the distance of the new trajectory from the facility. As with any major public work an Environmental Impact Assessment (EIA) had to be filed with the various authorities who jointly were financing the project. It has been asked that a Quantitative Risk Assessment (QRA) be included in the EIA to support the choice of the trajectory of the new highway around the refinery. Various

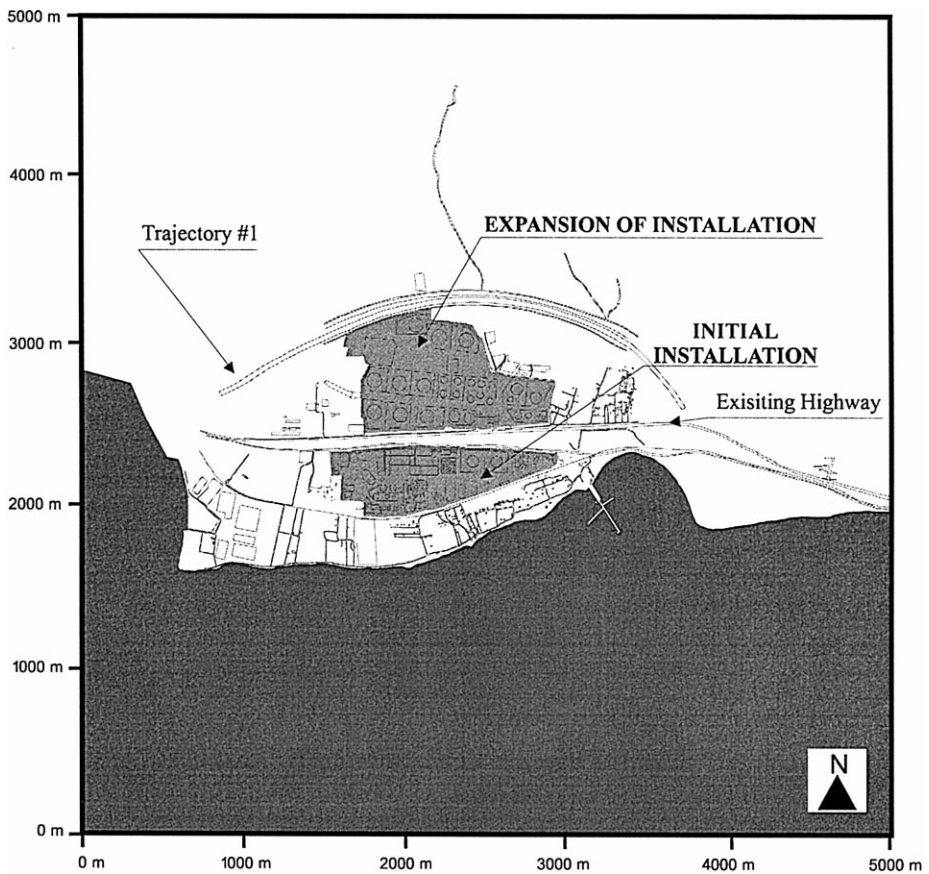

Fig. 1. Area under study.

refinery products are stored in the tank farm including: (a) *Fuel oil* in cylindrical floating-roof tanks with diameter up to 90 m; (b) *Jet fuel* and *gasoline* in cylindrical floating-roof tanks with diameter up to 70 m; (c) *Liquefied Petroleum Gas* (LPG) in spherical tanks with diameter up to 16 m. An installation storing flammable materials represents a hazard because there is a possibility for accidents causing violent phenomena (explosions and fires) with a potential for detrimental effects to the safety of the workers and the public, as well as for property damage.

The physical characteristics of the phenomena following the release of flammable materials to the environment have been studied and modeled extensively [1–6]. In addition to flammable materials, as part of the refining process Hydrogen Fluoride (HF), a toxic material, is used as catalyst. The contribution to the risk of this material has been calculated and found negligibly small when compared to the risk of flammable materials. For this reason this paper presents only the QRA aspects of flammable materials. Based on the understanding of the physical models involved, a number of codes have been developed recommending minimum distances between vessels containing flammable materials and other important buildings and public ways, as for example, the NFPA code for Flammable and Combustible Liquids [7]. Their recommendations are, however, based on deterministic criteria. This paper presents an approach that aims at quantifying the risk to which the users of the highway are exposed. Procedural and methodological steps for performing QRAs in chemical installations are given in Refs. [8,9]. A similar approach but for the 'reverse' problem has been presented in Ref. [10], where the risks to the public from the transport of dangerous goods such as flammable substances is estimated. It is believed that the risk approach offers a self consistent and common platform where the possible consequences of different accidents can be combined and thus it offers a useful framework for supporting relevant decisions.

Section 2 outlines the basic procedural and methodological steps of QRA for installations handling flammable materials. Section 3 presents the application of the methodology outlined in Section 2 to the reference facility. Section 4 contains the calculations of risk measures for highway users. Finally, Section 5 presents the results and conclusions of the case study, while the models used in QRA are given in Appendix A.

2. QRA methodology for flammable materials

2.1. Methodological and procedural steps

The methodology and the procedures followed for a QRA of a chemical installation (handling a hazardous substance) can be divided in the following 10 major steps.

2.1.1. Hazard identification

The main potential sources of hazardous-substance releases are identified and the initiating events that can cause such releases are determined.

2.1.2. Accident sequence modeling

A logic model for the installation is developed. The model includes each and every initiator of potential accidents and the response of the installation to these initiators. Specific accident sequences are defined which consist of an initiating event, specific system failures or successes and their timing, and human responses. Accident sequences eventually result in the release of the hazardous substance. Accident sequences resulting in the same failure mode of the installation are grouped into plant damage states (e.g. tank failure from overpressure).

2.1.3. Data acquisition and parameter estimation

In this step all necessary data for quantifying the models developed in the previous step are gathered and processed.

2.1.4. Accident sequence quantification

This step quantifies the accident sequences, that is, calculates their frequency of occurrence.

2.1.5. Assessment of hazardous-substance release categories

Release categories of the hazardous substance are defined in order to streamline the calculation of the consequences of the accidents and the associated frequencies. A release type uniquely determines all the qualitative and quantitative installation-depended aspects of the release that are necessary for the calculation of the consequences. In general this comprises the quantity and the physical conditions of the released hazardous substance and the associated physical phenomena. For example, a release type determines: the quantity, pressure, temperature, density etc. of the released substance; whether the release is continuous or instantaneous; whether the release is in the gaseous or liquid phase; whether an evaporating pool is formed; whether the vapor is forming a plume heavier or lighter than air and so on. In the case of LPG, a release type determines whether a violent phenomenon like BLEVE (Boiling Liquid Expanding Vapor Explosion) will occur or whether the gas is going to be dispersed and under what conditions.

A plant-damage state (defined in step 4 above) might result in a certain probability for a number of different release categories. The objective of this step is to determine the various release types and their conditional (on each plant damage state) probabilities of occurrence.

2.1.6. Extreme phenomena modeling

For flammable materials this step consists of establishing appropriate models for simulating the heat radiation or the overpressure resulting from the possible ignition of a released quantity of these materials and the phenomenon that follows it.

2.1.7. Dose and consequence assessment

The ‘dose’, that is the exposure of an individual to the extreme phenomenon, integrated over time, is calculated. Any emergency response plans or other mitigating actions are taken into account at this point. Appropriate dose–response models receiving

as input the dose of heat radiation or overpressure and providing the vulnerability of the receptor of the dose to a particular harm are established.

2.1.8. Data acquisition and parameter estimation for consequences

As in the case of step #3, all necessary data for quantifying the consequence models are gathered and processed to yield values for the parameters of these models. Alternatively, values of certain parameters are retrieved from the literature.

2.1.9. Consequence quantification

All models developed in step #6 are quantified using the values of the parameters developed in step #7. Quantification of uncertainties is also performed in this step.

2.1.10. Integration of results

Integration of the analysis performed in the previous steps allows the range of possible consequences and the associated uncertainties to be established. This set of doublets (consequence level, probability of occurrence) constitutes the most general form of risk quantification. However, the two indices of risk that are used in decision making are: (a) the *individual risk* $R(x,y)$ referring to the probability per year (frequency) of death of an individual staying at point (x,y) as a result of the exposure to the intense phenomena, and (b) the *group risk* $f(N)$ referring to the probability per year (frequency) of a single accident resulting in a number of deaths exceeding N.

Details of the methodological steps 1–5 for the case of an installation storing toxic material are given in Ref. [11]. Details for steps 5–10 for toxic materials are also given in Ref. [12]. The analysis presented here concentrates on steps 5–9 and the associated methodology is specific to the analysis of flammable materials (see also Ref. [13]). Plant damage states and corresponding frequencies of occurrence are assumed known.

2.2. Quantitative framework for risk assessment

This section presents the quantitative framework associated with the methodological and procedural steps presented in the previous section and followed in the analysis presented in this paper. Let

d	be an index spanning the possible plant-damage states determined for the installation: $(d = 1,\ldots, D)$
D	be the total number of plant damage states
f_d	be the frequency of plant-damage state d
k	be an index spanning the possible release categories of hazardous materials determined for the installation: $(k = 1,\ldots, K)$
K	be the total number of release categories
p_{dk}	be the conditional probability that release category k will occur *given* that plant-damage state d has occurred
$q_k(x,y,t)$	be the intensity of the extreme phenomenon at location (x,y) and at time t generated by release category k.

Health consequences do not depend only on the intensity of the adverse phenomenon following the release of hazardous material but also on the duration for which an individual is exposed to this extreme phenomenon. The extent of damage that a phenomenon might cause depends on a combination of its intensity and its duration. A measure that can depict this combination is *dose* and makes possible the comparison of exposures differing both in their intensities and in their duration. Let:

$\dot{D}_k(x,y,t) = f[q_k(x,y,t)]$ denote a function of the intensity, characteristic of the nature of the phenomenon, determining the *dose rate* at point (x,y) and at time t

T denote the duration of the phenomenon

$D_k(x,y)$ denote the *dose* of a receptor at the point (x,y) with respect of the location of the source owing to the phenomenon generated by release category k.

Then, dose is determined by

$$D_k(x,y) = \int_0^T \dot{D}(x,y,t)\,\mathrm{d}t \tag{1}$$

Two different exposures characterized by the same dose are then considered equivalent with respect to the harm they refer to. It follows that the concept of dose allows the comparison of phenomena characterized by the same mechanism of harm (e.g. thermal radiation).

Although the concept of dose allows for the comparison of different accidents involving the same type of intense phenomenon it does not allow for comparison of events resulting in undesired consequences through different mechanisms. Even for dispersion and later ignition of LPG a total figure of merit for the resulting consequences cannot be obtained on the basis of dose since dose of overpressure cannot be compared to dose of thermal radiation.

A common basis allowing combination and/or comparison of doses of different phenomena is the impact that each dose has on the sensitive receptor, in this case the human health. Such a figure of merit is the individual risk. Individual risk of death is defined as '*the probability that an individual in the vicinity of the facility will die as a result of an accident in the facility*'. In general the probability of an individual fatality depends on the dose of the exposure to the severe phenomenon that follows the release of the hazardous material. The relationship between the dose and the probability of death is determined for empirical data and is normalized through the so called Probit function as follows [14].

$$Y = A + B\ln\left[D_k(x,y)\right] \tag{2}$$

$$R_k(x,y) = \frac{1}{\sqrt{2\pi}}\int_{-\infty}^{Y-5} \mathrm{e}^{-u^2/2}\,\mathrm{d}u \tag{3}$$

where

Y denotes the Probit function of the dose

A, B are constants characterizing the phenomenon

$R_k(x,y)$ is the probability of death for an individual that has received a dose $D_k(x,y)$.

Once all these quantities have been defined and calculated the overall individual risk at a point (x,y) in the neighborhood of the installation can be determined as follows.

$$R(x,y) = \sum_{d=1}^{D} f_d \sum_{k=1}^{K} p_{dk} R_k(x,y) \quad (4)$$

This general approach is exemplified and applied in the installation under consideration in the following sections.

2.3. Plant damage states for hydrocarbon storage facilities

The installation under analysis consists of storage facilities containing the following substances.

2.3.1. Liquefied Petroleum Gas (LPG)

Stored under pressure in large spheres ranging in capacity from 500 to 3000 m^3. There are three basic types of damage states for these facilities that can lead to accidents.

2.3.1.1. Break in the LPG sphere and delayed ignition of LPG. This plant damage state resulting in release and dispersion of the LPG, incorporates all the accidents that may lead to a loss of the pressure boundary and subsequent release of the LPG which is further dispersed and possibly ignited giving rise to a *UVCE* or a *flash fire*, as it is described in Sections 2.4 and 2.5. Examples of such failures include failure of the sphere shell or piping, a valve failed to open, etc.

2.3.1.2. Jet fire impinging on the LPG sphere. This particular damage state has the potential for weakening the metal shell of the sphere with subsequent failure and occurrence of a BLEVE. This phenomenon is also further explained in Section 2.6.

2.3.1.3. Break in the LPG sphere and immediate ignition of the LPG. This plant damage state results in the escape of liquefied gas from the pressurized storage, which owing to the high outflow speed leads in forced mixing and a turbulent free jet. Whenever such a mixture is ignited, this will produce a *jet fire*, as explained in Section 2.7.

2.3.2. Crude oil

Stored in Floating Roof Cylindrical Tanks with a capacity of 120 000 m^3 under atmospheric conditions. The basic plant damage state for this case, described in Section 2.8, is the following.

2.3.2.1. Break in the oil-storage cylindrical tank. This damage state includes all accidents leading to the release of the oil in the dike surrounding the tank.

2.3.3. Hydrogen Fluoride (HF)

Stored under pressure in tanks of the alkylation unit, where it is used as catalyst. Although the contribution to the risk from this material has been calculated, details are

not given here since the effect is negligible compared to that of the flammable material (see Section 3). Details of QRA for toxic materials are given in Refs. [11,13].

2.4. Release categories following a break in the LPG sphere

A release category for LPG dispersion is defined in terms of all the conditions and parameters that uniquely determine the concentration of LPG at any point in space and at any instant of time following the release.

In this application it has been assumed that the size of the break in the sphere will be such that there will be a *continuous or instantaneous release* of gas in the atmosphere (see branch #1–8 of Fig. 2) which in turn will behave as a gas *heavier than air* over a flat terrain and that the total amount of LPG in the sphere will be released. Given these two basic assumptions, the other conditions and parameters determining the dispersion behavior of the gas are:

The rate at which it is released, and the meteorological conditions, namely:
Ambient Temperature
Stability Class
Wind speed
Wind direction

All these parameters are characterized by uncertainty. The first one because of uncertainties that characterize the exact conditions of the damage (nature, size and location of break, duration of release and measures to stop it) and the latter four because of actual weather variability at the site. Quantification of these uncertainties has been achieved by considering the parameters as random variables, each associated with a particular probability density function (pdf). In addition, the last four variables are correlated according to the results of a statistical analysis of weather data from the particular site.

Since each of the five parameters can take any value in a range of possible values, it follows that there is a very large number of release types resulting from the Cartesian product of the five subsets. Furthermore, the release type that will obtain following a break in the continuity of the pressure boundary of the sphere is also characterized by uncertainty since it is determined in terms of uncertain quantities. In order to simulate this uncertainty a sample of 100 release types has been generated each consisting of a particular combination of the five random variables. The sample has been generated according to the Latin Hypercube Sampling procedure [15].

The sequence of events following the damage to the installations are schematically outlined in the event tree given in Fig. 2 and described in the following subsections.

2.5. Consequence assessment for LPG dispersion

Once released, the LPG represents a hazard because it might ignite and cause an intense phenomenon. If the ignition is not immediate (see Fig. 2, branches #2, #3, #6, #7), the LPG will disperse, and it will mix with air forming a combustible mixture. If this mixture meets an ignition source it may ignite. For an ignition to take place the

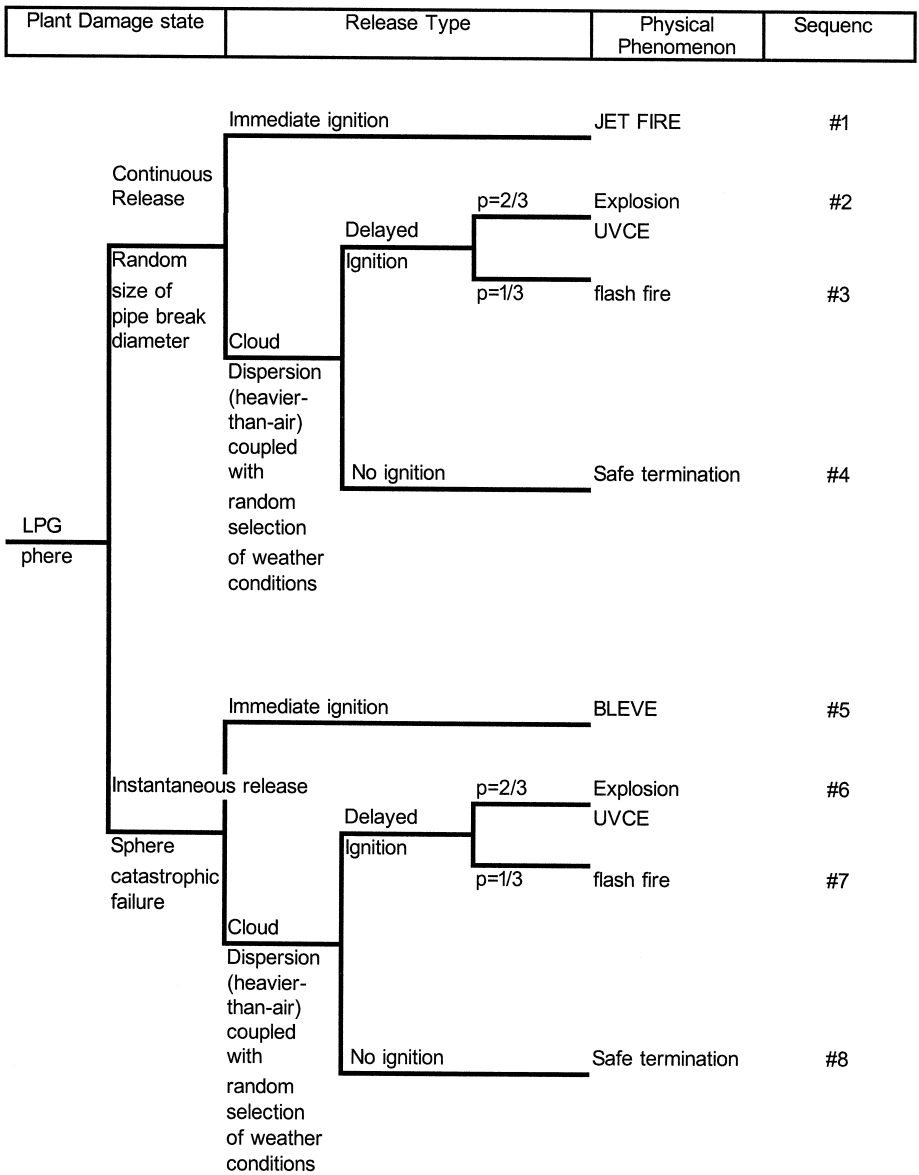

Fig. 2. Post-accident sequences of LPG storage spheres.

concentration of the cloud at the point of ignition must be between the lower flammability limit (LFL) and the upper flammability limit (UFL).

Given a particular release category, (i.e. amount of LPG released, the rate at which it is released, the temperature, the stability class, and the wind speed and direction), the

LPG is assumed to be dispersed according to the physical model for the dispersion of a gas heavier than air over flat terrain incorporated in the computer code SOCRATES and outlined in Ref. [13]. This model is based on the models in Refs. [16–18]. For a given release category, the dispersion model provides the location of the cloud, that is, the concentration at each point in space and time. As a result at each instant of time the 'trace' of the flammable cloud (points with concentration between UFL and LFL) is known. If at this instant an ignition takes place one of two phenomena, namely explosion or a flash fire, will take place [19,20] (see Fig. 2, branches #2, #3, #6, #7).

The location of the ignition sources has been assumed randomly distributed around the site. In particular a uniform distribution of ignition sources as a function of the distance from the installation center has been considered.

For each release, the upper and lower flammability distances are determined and compared to the randomly selected distance of the ignition source. If this latter distance falls within the flammable region an explosion is assumed to take place the moment the front of the cloud reaches the ignition source. The mass involved in this explosion is equal to the total mass released up to this point. Specific models of these phenomena are given in Appendix A.

2.6. Release categories and consequences for LPG BLEVE

A fire in the vicinity of a sphere storing LPG has the potential to create a very severe phenomenon called BLEVE (Fig. 2, branch #5). In order for a BLEVE to take place, the fire should last for about half an hour so that the heat produced can on the one hand weaken the metal shell of the spherical tank, and on the other result in a rise of the pressure of the gas [22]. The combined effect of these two actions could then cause a failure of the sphere, releasing violently the liquefied gas which is ignited forming a large *fireball*. The intense thermal radiation of this fireball can reach significant distances [20,22]. The model used for this phenomenon is also presented in Appendix A.

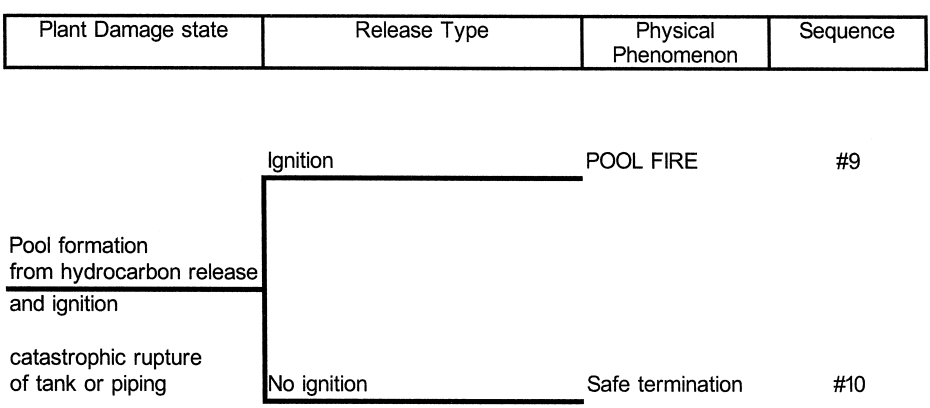

Fig. 3. Post-accident sequences of liquid hydrocarbon storage spheres.

2.7. Jet fire

Instantaneous ignition of a pressurized release of LPG exiting an orifice (see Fig. 2, branch #1) will result in a jet fire, which is also described in Appendix A.

2.8. Release categories and consequences for an oil fire

Ignition and burning of oil stored in cylindrical tanks with floating roofs is relatively difficult since this particular storage system minimizes the vapor phase in the tank. If, however, for some reason (e.g. an earthquake) there is a break in the tank followed by release of the oil in the dike surrounding the tank, it is possible to have ignition and burning of the oil forming a *pool fire*. This accident structure is shown in Fig. 3, while an appropriate model is given in Appendix A.

3. QRA of the tank farm

A QRA for the tank farm of the oil refinery has been performed according to the methodology outlined in the previous sections using the computerized set of QRA tools SOCRATES [13].

A total of 82 plant-damage states have been considered describing various types of accidents in the different pieces of installation as shown in Table 1. For each plant damage state an individual risk profile (i.e. individual risk values for each point of the study area) has been calculated and the 82 profiles were combined according to Eq. (4) into a single overall individual risk profile.

For each plant-damage state 100 release categories have been considered. Each release category is determined by a random selection of the value of the various uncertain variables that determine it. Table 2 provides, for each generic type of plant damage state, the parameters that have been considered as random variables along with the probability density functions that quantify the uncertainty about them. Discrete probability distributions have been considered for the equivalent break diameter with four possible values of each type of storage tanks. Weather variability has been taken into account by considering variable wind direction. For each wind direction a conditional continuous pdf for wind velocity has been considered, while a discrete distribution is assumed for each of the six possible Pasquil–Guifford stability classes. All distributions were derived by fitting the relevant data from a weather station near the site. For each plant damage state an individual risk profile, conditional on this particular plant-damage state having occurred, has been generated. The conditional individual-risk profile for the BLEVE plant-damage state in a 3000 m^3 butane sphere is shown in Fig. 4, while the corresponding profile for the UVCE plant-damage state of the same sphere is shown in Fig. 5.

Eighty-two conditional individual risk profiles have been generated and combined according to Eq. (4) into the overall individual risk profile shown in Fig. 6. The

Table 1
Plant damage states used in the risk assessment of the refinery

Index of plant damage states	Number of tanks	Consequence model	Substance	Characteristic size	Single accident frequency
1	1	BLEVE	propane	500 m^3	0.8e−6/year
2	1	Sphere catastrophic rupture instantaneous ignition (jet fire)	propane	500 m^3	2.5e−6/year
3	1	Sphere catastrophic rupture delayed ignition explosion (UVCE)	propane	500 m^3	1.7e−6/year
4	1	Sphere catastrophic rupture delayed ignition (flash fire)	propane	500 m^3	0.8e−6/year
5	1	BLEVE	propane	2500 m^3	0.8e−6/year
6	1	Sphere catastrophic rupture instantaneous ignition (jet fire)	propane	2500 m^3	2.5e−6/year
7	1	Sphere catastrophic rupture delayed ignition explosion (UVCE)	propane	2500 m^3	1.7e−6/year
8	1	Sphere catastrophic rupture delayed ignition (flash fire)	propane	2500 m^3	0.8e−6/year
9	1	BLEVE	butane	500 m^3	0.8e−6/year
10	1	Sphere catastrophic rupture instantaneous ignition (jet fire)	butane	500 m^3	2.5e−6/year
11	1	Sphere catastrophic rupture delayed ignition explosion (UVCE)	butane	500 m^3	1.7e−6/year
12	1	Sphere catastrophic rupture delayed ignition (flash fire)	butane	500 m^3	0.8e−6/year
13–14	2	BLEVE	butane	2500 m^3	0.8e−6/year
15–16	2	Sphere catastrophic rupture instantaneous ignition (jet fire)	butane	2500 m^3	2.5e−6/year
17–18	2	Sphere catastrophic rupture delayed ignition explosion (UVCE)	butane	2500 m^3	1.7e−6/year
19–20	2	Sphere catastrophic rupture delayed ignition (flash fire)	butane	2500 m^3	0.8e−6/year
21–22	2	BLEVE	butane	3000 m^3	0.8e−6/year
23–24	2	Sphere catastrophic rupture instantaneous ignition (jet fire)	butane	3000 m^3	2.5e−6/year
25–26	2	Sphere catastrophic rupture delayed ignition	butane	3000 m^3	1.7e−6/year
27–28	2	Sphere catastrophic rupture delayed ignition (flash fire)	butane	3000 m^3	0.8e−6/year
29–34	6	Pool fire 70	fuel oil	160 m	1.0e−5/year
35–41	7	Pool fire 30	fuel oil	80 m	1.0e−5/year

Table 1 (continued)

Index of plant damage states	Number of tanks	Consequence model	Substance	Characteristic size	Single accident frequency
42–47	6	Pool fire 40	fuel oil	90 m	1.0e−5/year
48–56	9	Pool fire 90	fuel oil	170 m	1.0e−5/year
57–67	11	Pool fire 45	fuel oil	160 m	1.0e−5/year
68–72	5	Pool fire 20	fuel oil	60 m	1.0e−5/year
73–75	3	catastrophic rupture of drum HF toxic release	HF	small bore	0.53e−6/year
76–77	2	catastrophic rupture of drum HF toxic release	HF	full bore	1.0e−6/year
78–79	2	catastrophic rupture of drum under pressure HF toxic release	HF	full bore	5.0e−6/year
80	1	catastrophic rupture of drum in V-11101 instantaneous ignition	fuel oil	1400 kg/s	2.5e−6/year
81	1	catastrophic rupture of drum in V-11101 delayed ignition (UVCE)	fuel oil	1400 kg/s	1.7e−6/year
82	1	catastrophic rupture of drum in V-11101 delayed ignition (Flash fire)	fuel oil	1400 kg/s	0.8e−6/year

calculation of each individual-risk profile, as well as the combination into the overall profile was performed automatically by the SOCRATES computer program which has the capability to accept sources of different hazardous materials at different locations in a general area and also the capability to receive multiple damage-states for each source and combine the partial results [13].

An alternative representation of individual risk is given in Fig. 7, where the maximum individual risk as a function of the distance from the center of the installation is plotted. For example, the maximum individual risk at a distance of 1000 m from the 'center' of the installation equals to more than 10^{-5}/year. It follows that points at distances greater than 1000 m from the center of the installation are certain to be characterized by an individual risk of less than 10^{-5}/year. Hence, Fig. 7 can be also assumed as giving the distance (from the 'center' of the installation) beyond which individual risk will always be lower than a given level. Graphs like the one shown in Fig. 7 are of limited value giving only a qualitative sense of the relative importance of the various accidents since they do not adequately convey the importance of wind direction variability and the relative location of the various sources of risk. They can be used, however, in drawing general conclusions about the relative contribution of the various accidents to individual risk. It follows that a toxic hydrogen fluoride (HF) release from the processing refinery units (not presented in this work) has a minor contribution to the individual risk at any distance owing to the prevailing wind direction

Table 2
Probabilities for uncertain variables used in the risk assessment of the refinery

Wind velocity		Wind velocity distribution (lognormal, conditional on wind direction)		Probability of particular P–G stability class (condition on wind direction)					
Direction	Probability (%)	0.1% percentile	99.9% percentile	A	B	C	D	E	F
N	4	0.12	23.028	0.1	0.175	0.062	0.264	0.049	0.351
NNE	4	0.12	23.028	0.1	0.175	0.062	0.264	0.049	0.351
NE	2.5	0.128	23.007	0.099	0.174	0.062	0.269	0.053	0.343
NEE	2.5	0.128	23.007	0.099	0.174	0.062	0.269	0.053	0.343
E	1.1	0.116	16.317	0.103	0.18	0.046	0.248	0.04	0.383
SEE	1.1	0.116	16.317	0.103	0.18	0.046	0.248	0.04	0.383
SEE	5.05	0.149	19.713	0.119	0.191	0.059	0.228	0.063	0.34
SSE	5.05	0.149	19.713	0.119	0.191	0.059	0.228	0.063	0.34
S	5.3	0.145	16.937	0.153	0.192	0.051	0.192	0.056	0.356
SSW	5.3	0.145	16.937	0.153	0.192	0.051	0.192	0.056	0.356
SW	4.8	0.146	20.536	0.118	0.184	0.066	0.234	0.065	0.333
SWW	4.8	0.146	20.536	0.118	0.184	0.066	0.234	0.065	0.333
W	4.35	0.123	38.626	0.081	0.148	0.097	0.36	0.065	0.249
NWW	4.35	0.123	38.626	0.081	0.148	0.097	0.36	0.065	0.249
NWW	22.9	0.138	31.798	0.084	0.158	0.084	0.327	0.064	0.283
NNW	22.9	0.138	31.798	0.084	0.158	0.084	0.327	0.064	0.283

Propane tanks rupture equivalent diameter (mm)	Probability	Butane tanks rupture equivalent diameter (mm)	Probability
620	0.1	800	0.1
200	0.6	400	0.6
100	0.2	200	0.2
50	0.1	100	0.1

(note the logarithmic scale in the individual risk axis) while pool fires dominate at short distances with the BLEVE of the large LPG spheres taking the dominant role in large distances.

4. Risk measures for highway users

4.1. Individual risk for highway users

Individual risk in Section 2.2 and Eq. (1) has been calculated under the assumption that the individual remains at the same location (x,y) for the duration of the phenomenon, while the intensity of the extreme phenomenon may vary. An equivalent

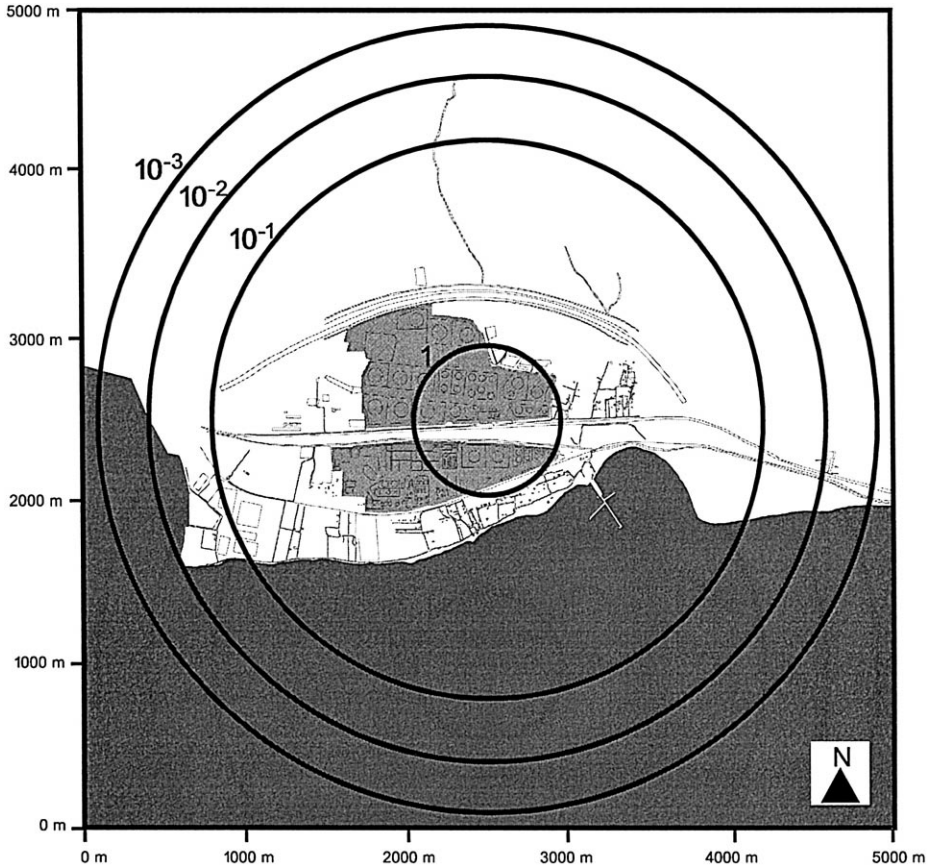

Fig. 4. Conditional Individual Risk contours for the BLEVE plant-damage state in a 3000 m^3 butane sphere.

situation arises when the individual does not remain in the same location but instead it is moving in a field where the intensity of the unwanted phenomenon changes from one point to another regardless of whether the intensity varies or not with time. It must be noted that only direct effects of a hazardous release on road users are being considered, as secondary effects, like smoke leading to poor visibility or collision with a vehicle overturned as a result of a blast explosion, are similar to all different trajectories and hence are not differentiated.

Let us suppose, for example, that an individual is moving following a trajectory determined by the equation

$$x = f_1(x_0, y_0, t),\ y = f_2(x_0, y_0, t) \tag{5}$$

This means that given the initial position (x_0, y_0) the coordinates (x, y) of the individual are given by Eq. (5) at each instant of time. Since the individual is moving,

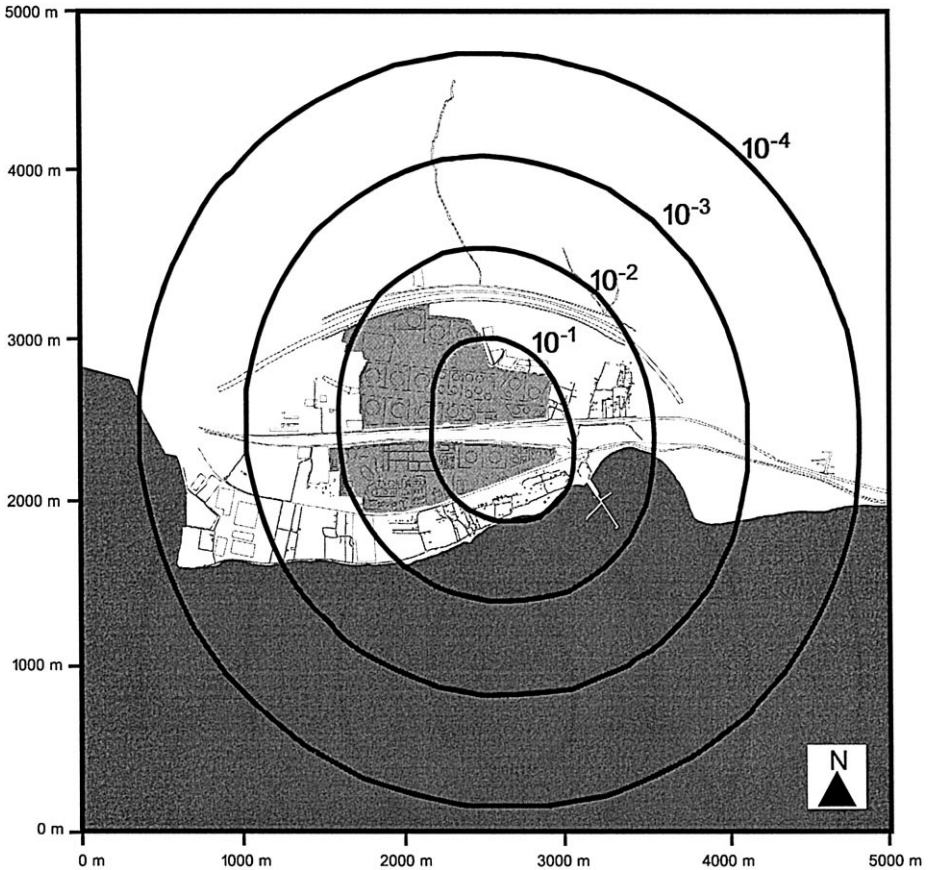

Fig. 5. Conditional Individual Risk contours for the UVCE plant-damage state in a 3000 m^3 butane sphere.

individual risk cannot be associated with a fixed point in space (x,y) anymore. It can, nevertheless, be associated with the *initial position* (x_0,y_0) of an individual. In this case Eq. (1) becomes

$$D(x_0,y_0) = \int_0^T \dot{D}(x,y,t)\,\mathrm{d}t$$

or

$$D(x_0,y_0) = \int_0^T f[q(x,y,t)]\,\mathrm{d}t \rightarrow$$

$$D(x_0,y_0) = \int_0^T f\{q[f_1(x_0,y_0,t), \quad f_2(x_0,y_0,t),t]\}\,\mathrm{d}t \tag{6}$$

In the case of the highway, an individual moves on the highway trajectory with speed v equal to the speed of the car it is riding on. Eq. (6) can then be solved as follows.

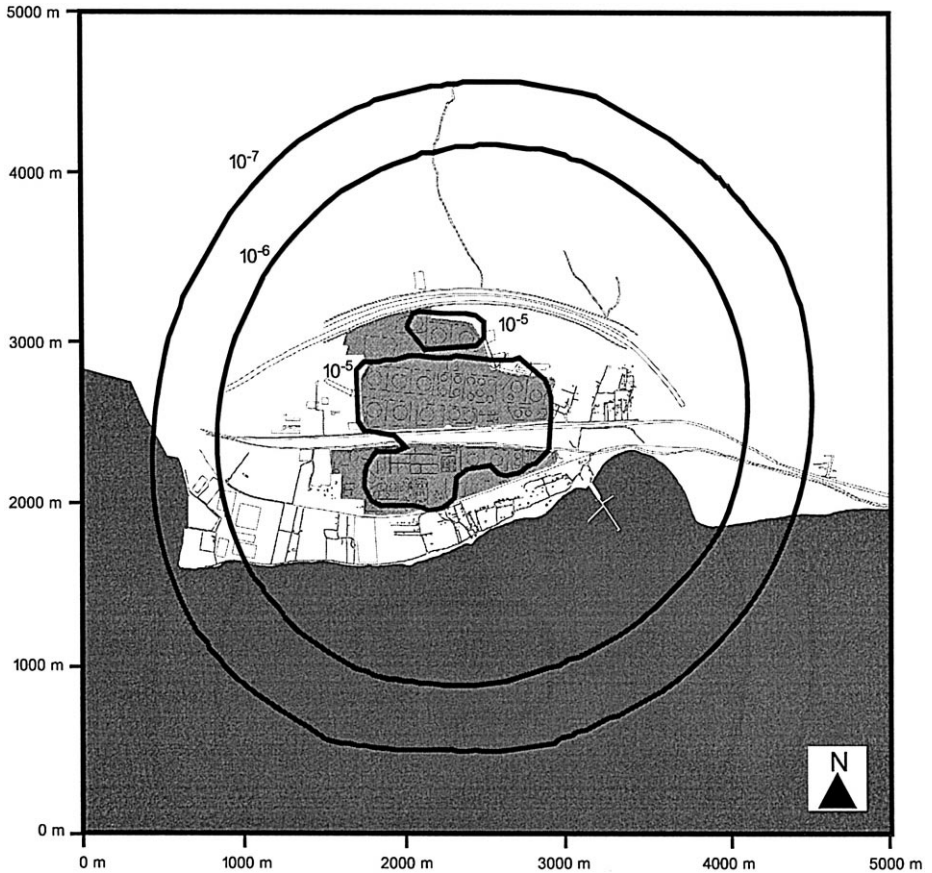

Fig. 6. Total Individual Risk contours.

The section of the highway within the area of analysis and in each direction of movement has been divided into a number of segments, each of length s. The time it takes an individual to travel each segment is given by

$$\Delta t = \frac{s}{v} \tag{7}$$

Eq. (6) then becomes

$$D_j = \sum_{i=j}^{j+M} f\left[q(x_i, y_i)\right]\Delta t \tag{8}$$

$$M = \frac{Tv}{s} \tag{9}$$

where

(x_i, y_i) the coordinates of the ith segment

(x_j, y_j) the coordinates of the jth segment where the individual is found at the onset of the accident

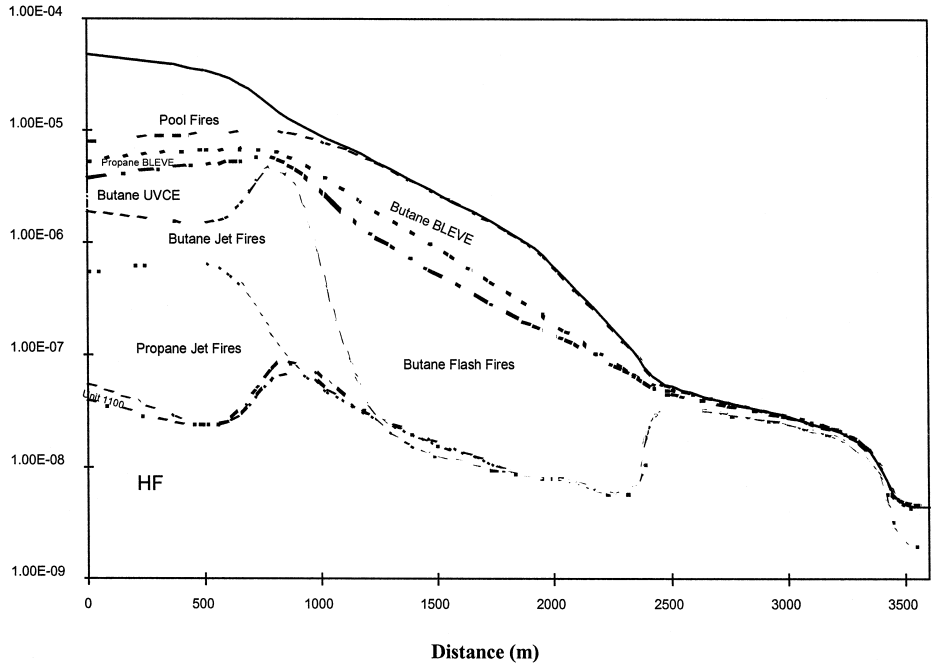

Fig. 7. Maximum Individual Risk vs. distance and absolute contribution of each release category.

$q(x_i, y_i)$ the intensity of the phenomenon at point (x_i, y_i) assumed constant during the $(i, i+1)$ time interval
T duration of the phenomenon
v speed of vehicles in the highway
s length of individual highway segment
M duration of phenomenon in time steps of duration Δt.

Eq. (8) provides the dose received by an individual moving along the highway and being in the jth segment at the onset of the phenomenon. Both directions of movements have been considered (east–west and west–east) and the counting in Eq. (8) is performed along the direction of movement. This distinction was made to take into account the fact that, depending on the accident, vehicles moving in one direction might be moving toward points of greater intensities (e.g. heat radiation) while vehicles moving in the opposite direction might be moving toward lower intensities.

This procedure creates a series of risk indices R_{dj} $(d = 1, \ldots, D,\ j = 1, \ldots, J)$ for each direction of movement where d refers to one of the 82 plant-damage states and j to one of the 50 segments. Overall individual risk can be obtained according to

$$R_j = \sum_{d=1}^{D} f_d R_{dj} \tag{10}$$

yielding unconditional on the plant-damage state individual risk for each segment j of the highway.

Three alternative trajectories for the highway have been considered: (1) Existing Highway, that is the road passing through the refinery (see Fig. 1); (2) Trajectory #1 bypassing the refinery but at the border of the refinery (see Fig. 1); and (3) Trajectory #2 being parallel to trajectory #1 and at distance of 100 m away from the refinery.

Fig. 8 gives the individual risk profile for each of the three trajectories and for both directions of movement (east–west and west–east). As can be seen, individual risk of the existing highway is higher than that for trajectory #1 which in turn is higher than that for trajectory #2 for each segment and for both directions of movement. This is a rather expected result given the relative distance of each trajectory from the various hazard sources.

A certain degree of asymmetry in the individual risk profile for the two directions of motion in the existing road is due to the asymmetry of the position of the various hazard-sources with respect to the road. This asymmetry is not that important as the trajectory moves away from the center of the refinery.

Consideration of the individual risk profiles of the various trajectories provide a clear indication that, with respect to this criterion, trajectory #1 represents a clear improvement over the existing road, bringing the level of maximum individual risk from 1×10^{-5}/year down to about 4×10^{-6}/year. Trajectory #2 on the other hand offers only a marginal improvement reducing the maximum individual risk down to about 3×10^{-6}/year.

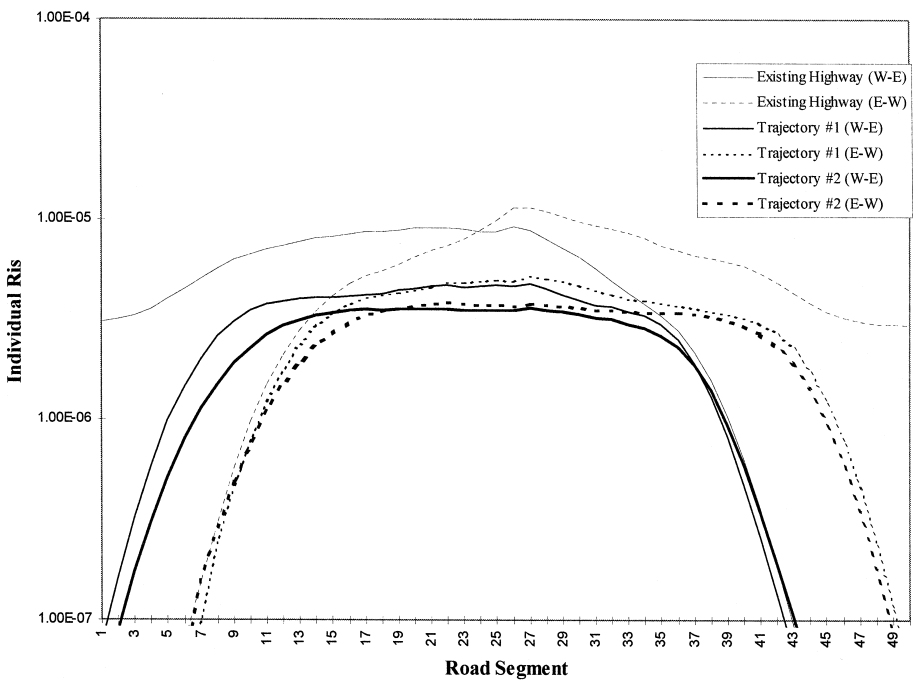

Fig. 8. Individual Risk for all road trajectories for both directions.

4.2. Group risk for highway users

Group risk is a risk measure referring to the number of people that can be affected by an accident. Formally, group risk is defined as the probability that, as a result of a single accident, a group of receptors equal or larger than N will suffer a particular damage. In this application the receptors of interest are the users of the highway and the damage is loss of life.

Given its definition, group risk is expressed in terms of the complementary cumulative distribution function (CCDF) of the random variable 'number of fatalities'. When graphed the CCDF is also referred to as 'F–N' curve. The CCDF of a random variable N gives the probability that the random variable will take a value greater or equal to N. The individual risk to which any individual is exposed constitutes one of two necessary inputs to the calculation of group risk, the second being the size of the population exposed to the risk.

The number of people using the highway at a given instant of time is calculated on the basis of the division of the highway into elementary sections as follows:

$$n = \frac{sl\varepsilon}{v}, \tag{11}$$

where

s length of elementary section of highway (km)
l traffic load (cars/h)
v car speed (km/h)
ε number of passengers per car

Since the individual risk of each segment j is known (for each direction of movement), that is, the probability with which each individual will die is R_{dj} and there are n individuals in each segment, the number of people x_{dj} to be killed in this segment as a result of an accident d follows the binomial distribution that is

$$g(x_{dj}) = \binom{n}{x_{dj}} R_{dj}^{x_{dj}} (1 - R_{dj})^{n - x_{dj}} \tag{12}$$

It is noteworthy that the expected value of x_{dj} is equal to nR_{dj} which is sometimes used as a measure of the group risk.

Given that there are $2J$ segments (J in each direction) the total number of people that can be killed as a result of a single accident is given by the sum of the $2J$ elementary segment numbers.

$$\tilde{N}_d = \sum_{j=1}^{2J} \tilde{x}_{dj} \tag{13}$$

where each $\tilde{x}_{dj}$ is distributed according to Eq. (12).

Given relationships (12) and (13), the CCDF of the total number of people killed in the highway as a result of the dth accident, $F_d(N)$, can be calculated numerically. Finally, the overall 'F–N' curve unconditional on the particular accident is given by

$$F(N) = \sum_{d=1}^{D} f_d F_d(N) \tag{14}$$

where f_d is the frequency of occurrence of the dth damage state (see Table 1)

A number of remarks concerning the parameters in Eq. (11) are given below. In general, the traffic load l depends on the time of the day, day of the week and week of the year. The same is true for the number of passengers per car and the speed of the car v while v is, in addition, negatively correlated with the traffic load l. Since the individual risk R_{dj} has been assumed constant with time i.e. independent of the time of day, day of the week, season, etc. it follows from Eq. (12) that explicit time dependence on l, v, ε is not necessary. It is sufficient to consider the overall variation of l, v, ε through appropriate pdf's describing the stochastic and temporal variability of these variables. This way, the probability that, for example, the load will take a value in the interval $[l_1, l_2]$ expresses the percentage of time of a time-cycle (e.g. a year) during which the load has values in this interval if the load is deterministically known as a function of time. In the opposite case, the considered pdf contains, in addition to temporal variations, elements of random variation. Given historical traffic data from the existing highway, as well as, traffic analyses and growth projection, the variation of the traffic load has been simulated by a lognormal distribution with a 99% interval [3950 cars/day, 33 500 cars/day] (see also Fig. 9). The speed with which vehicles are moving in the existing highway has been found (through analysis of existing data) to follow a lognormal distribution with a 99% interval [52 km/h, 95 km/h]. To accommodate for

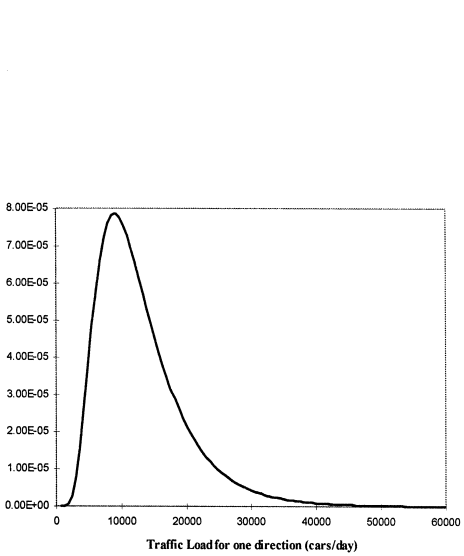

pdf of Traffic load for all trajectories

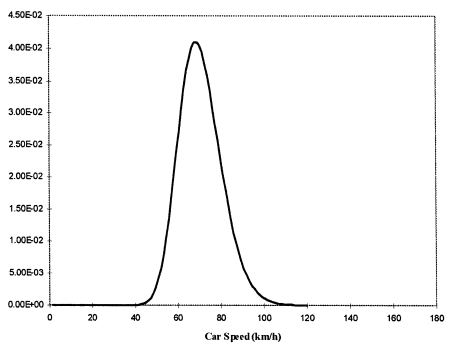

pdf of car speed for existing highway

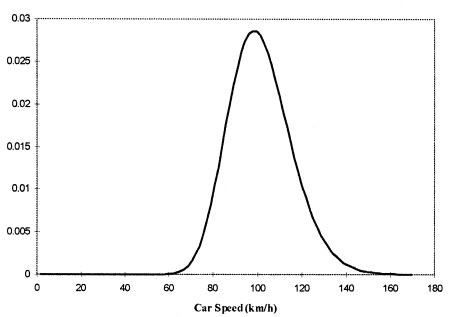

pdf of car speed for Trajecories #1 and #2

Fig. 9. Probability Density Functions for car load and car speed.

the design, size, and construction improvements associated with the new highway, the speed of the vehicles in the new road (trajectory #1 or trajectory #2) has been assumed lognormally distributed with a 99% interval [75 km/h, 135 km/h] (see Fig. 9). To accommodate the fact that heavy traffic loads are associated with low speeds, a high negative correlation between l and v has been used. Furthermore, a very strong negative correlation between traffic loads along the two opposite directions of traffic has been considered to take into account the 'rush-hour' effect where very heavy traffic in one direction is coupled with light traffic in the opposite direction. The specific types and parameters of the pdf's were based on data and projections of the public authority in charge of the highway design and construction.

The stochastic variability in the parameters l, v, ε has been taken into consideration as follows. A random sample for $\{l, v, \varepsilon\}$ has been generated and for each sample point the expected CCDF $F(N)$ has been developed according to Eqs. (11) and (12).

An example of such a calculation is given in Fig. 10, where the expected value of the CCDF for the number of fatalities owing to a BLEVE in the 3000 m^3 butane sphere is plotted for the three alternative trajectories. The three curves are very close together indicating that the three trajectories do not differ significantly with regards to the group risk from BLEVE in the 3000 m^3 butane sphere. In fact, trajectory #2 is characterized by a higher level of group risk (for $N > 100$) than trajectory #1 although it is further away from the risk sources. This can be explained with the help of Fig. 4 although the reader is reminded that the individual risk profile used to perform the group risk

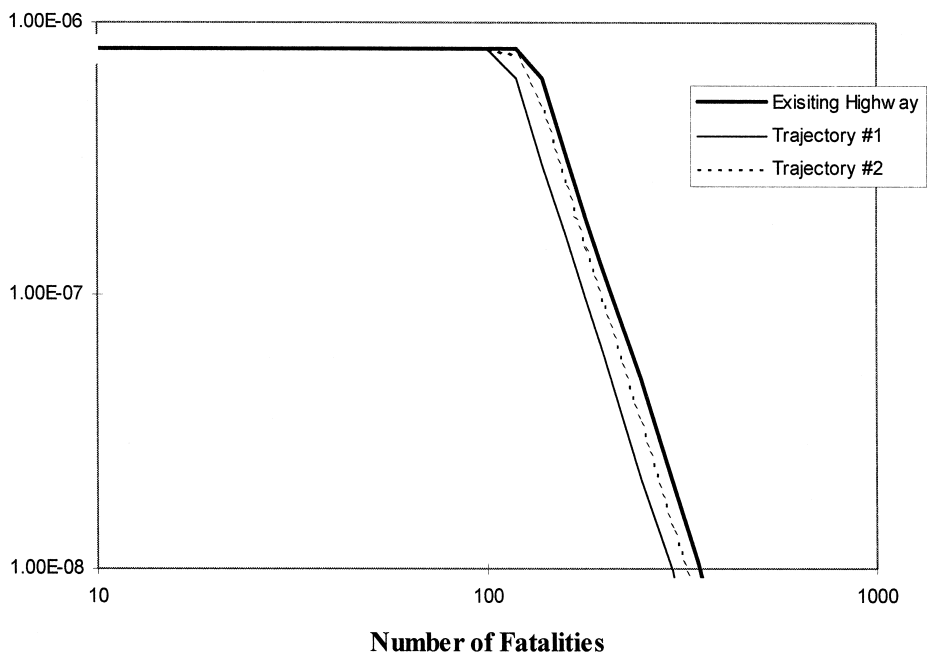

Fig. 10. $F-N$ curves owing to the 3000 m^3 sphere BLEVE accident for all trajectories.

calculations (referring to moving receptor) is slightly different than the risk shown in Fig. 4 (referring to a standing receptor, see also Section 4.2). Trajectory #2 runs parallel to trajectory #1 and 100 m away from the refinery. As it can be seen from Fig. 4, individual risk falls rather slowly from the 1 and 10^{-1} isorisk curves. As a result, the two trajectories are characterized by the same level of individual risk. This is true for every segment of each trajectory even after the more detailed calculations of Section 4.1. Trajectory #2 on the other hand, being 100 m away of trajectory #1 is characterized by a higher degree of curvature and hence by a greater length within the area of nonnegligible risk. As a result, trajectory #2 can accommodate more people than trajectory #1 at the same level of individual risk, hence the higher probability for an accident involving more than 100–500 people seen in Fig. 10.

Overall group risk results for the existing road and the two alternative trajectories are obtained from the 82 release-category CCDFs through Eq. (14).

The results (expected values of CCDFs) are shown in Fig. 11. It is noteworthy that the group risk of the existing road is higher than the two proposed trajectories at all levels of fatalities. At low levels (i.e. for $N < 100$) the group risk is mainly dominated by accidents with higher frequencies but lower consequences range (like pool fires and jet fires). Moving the road away from the center of the refinery reduces this contribution. At higher levels of fatalities (i.e. for $N > 100$) the contribution is mainly due to BLEVEs. Given the higher distance at which fatalities can occur, trajectories #1 and #2 do not represent a substantial improvement over the existing road. Actually trajectory

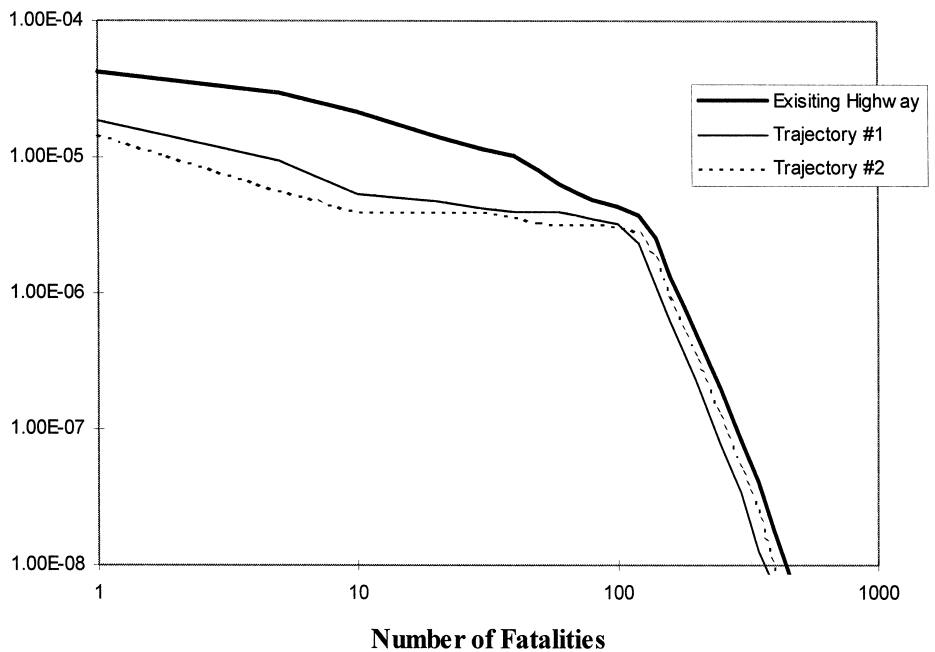

Fig. 11. Overall $F-N$ curves for all trajectories.

#2 seems more risky than trajectory #1 for larger levels of fatalities ($N > 100$) for the reasons explained earlier.

5. Summary and conclusions

A quantified risk assessment has been performed in order to provide input into a decision concerning the selection of a trajectory for a new highway in the neighborhood of an oil refinery.

A set of procedures and associated methodological steps have been developed and presented that allow for the quantification of risk of installations handling flammable materials. This approach allows for the calculation of two quantitative measures of risk, namely, the individual risk and the group risk.

Three alternative trajectories of a highway in the neighborhood of an oil refinery have been analyzed and two measures of risk, namely, individual risk along the length of the road and group risk, have been calculated for each trajectory. Individual and group risk have been calculated taking into account the results of the QRA as well as realistic assumptions about the movement of the vehicles on the highways, the traffic loads, the speed of the vehicles, the existing correlation factors among themselves and the direction of movement in the highway. Furthermore, additional uncertainties concerning conditions and consequences of accidents have been quantified.

A decision to bypass the refinery and build the new highway along trajectory #1 has been made by the appropriate authorities. The authors believe that the cost associated with moving the highway further away from the refinery owing to difficult terrain conditions was the overwhelming factor in making this decision. They also believe, however, that the QRA presented in this analysis helped in addressing a number of risk related issues. In this way, they consider the selection of the highway trajectory as being risk-informed.

First, the quantified risk analysis supported the intuitive qualitative argument that moving the road away from the center of the refinery is a risk-reducing action. The use of the individual risk measure allowed for the intercomparison of the effects of different accidents having higher frequencies of occurrence and lower range of consequences (like pool fires) along with accidents having low frequencies of occurrence and low range of consequences (e.g. BLEVE). The substantial degree of reduction in the individual risk from the existing highway to the new highway with trajectory #1 is mainly due to the elimination of the high frequency short range consequence accidents and not so much to the decrease of the consequences of the low frequency long-range consequence accidents. In this regard, consideration of only the most severe (consequence wise) accident (i.e. BLEVE) would have shown a much less significant differentiation between the three alternatives.

Second, the QRA helped quantify the effect of exposing groups of people of different sizes at different risk levels. This was made possible through the use of the group risk. Calculation of this risk measure helped illuminate the not immediately obvious result that trajectories further away from the risk source but in a region with relatively the

same level of individual risk are actually worse than trajectories closer to the source of risk, since the former accommodate a larger number of people.

In that respect, a trajectory passing directly through the center of the ground trace of a BLEVE fireball is less risky than one that traces the circumference of the isorisk with fatality probability equal to unity although the latter is located further away from the LPG tank.

Third, the analysis helped clarify the issue of whether the highway has been moved far enough so that the reduction at the individual risk level had compensated the increase in the number of people exposed at this risk owing to the increased capacity of the highway. Group risk measures taking into consideration different traffic loads and different vehicle speeds made that possible.

Fourth, all the calculations have been made taking into consideration existing uncertainties in the values of various parameters owing to stochastic variability and/or lack of complete knowledge, and not by ad hoc selection of single value parameters.

One aspect of the problem not explicitly addressed in this analysis was the potential of an accident in the highway causing an accident in the refinery through a domino effect. Given the possible range of consequences of an accident on the road (e.g. road tanker BLEVE) and the improved driving conditions in the new highway, it follows that the effect of moving the road to trajectory #1 will definitely decrease the frequency of the highway induced accidents in the refinery. On the contrary, there will be no significant change from trajectory #1 to trajectory #2 since the former is already far from the bulk of the hazard sources of the refinery. Quantification of this effect would further strengthen the conclusions of this analysis.

The overall conclusions of this analysis demonstrated that the selection of trajectory #1 represented an improvement over the existing situation from the risk point of view. Further substantial decrease in the risk would be achievable only if the trajectory were moved more than 1 km away from the refinery at an extremely high cost that was not justifiable by the decrease in the residual risk and at the same time prohibitive.

Acknowledgements

This work was partially supported by the Ministry of Environment, Public Works and Physical Planning of Greece and the Commission of the European Union through contract STEP No. CT90-0093 (TSTS).

Appendix A. Physical models for hydrocarbon releases

A.1. Unconfined Vapor Cloud Explosion (UVCE)

An ignition of a combustible mixture of a flammable gas and air may result in an explosion causing damage to the surroundings. The damage is mainly due to the shock wave that will be produced by such an Unconfined Vapor Cloud Explosion. Only the

part of the cloud with concentrations between the lower flammability limit (LFL) and upper flammability limit (UFL) will explode. The shock wave (overpressure) resulting from an UVCE can be calculated according to the relationships cited in Ref. [20]. The resulting overpressure is given by:

$$\frac{\Delta p}{p_0} = \phi \frac{L_0}{r} \tag{15}$$

with

$$L_0 = \left(m_{\mathrm{ex}} H_{\mathrm{c}} / p_0 \right)^{1/3} \tag{16}$$

where

Δp peak overpressure (Pa)
p_0 pressure (Pa)
ϕ factor depending on the 'reactivity' of the flammable material (flame velocity). For the LPG mixture it was taken to be [20] $\phi = 6 \times 10^{-2}$
L_0 'explosion length' (m)
r distance of the point from the 'center' of the cloud where the overpressure occurs (m)
m_{ex} mass of the flammable gas in the cloud (kg)
H_{c} heat of combustion (kJ/kg)

Given the trajectory of the flammable section of the cloud and the time of ignition the peak overpressure and the duration of the overpressure at a point located at a distance r from the center of the flammable cloud is given in terms of Eqs. (15) and (16). It follows that given the release category, the peak overpressure and the duration of the overpressure can be determined at each point (x, y) around the site of the pressurized sphere if the location at which the ignition takes place is known. This in turn, requires knowledge of the location of the possible ignition sources, their nature, and the time it takes to ignite the cloud. As mentioned before all uncertainties associated with ignition are incorporated into the time of ignition.

A.2. Flash fire

An alternative phenomenon resulting from the ignition of a combustible-mixture cloud is that of a flash fire where no explosion and hence no shock wave and overpressure is generated but instead, the flammable material is burned in a very short period of time.

In this case it has been assumed that an individual will be harmed only for those points inside the trace of the flammable envelope of the cloud. That is, it has been assumed that if an individual is found within this envelope at the instant of ignition, either standing or moving inside a vehicle, they will die, based on a simplistic model of Ref. [9]. It can be argued that an individual found at a point outside the flammable envelope and moving towards it, at the moment of the ignition, could get inside the fire

while the phenomenon is going on. The duration of the flash fire is, however, short enough so that this remark is valid for only a very short part of the highway and this effect is covered by the quantification of the uncertainties characterizing the release.

A.3. Dose assessment for UVCE and flash fire

Unconfined vapor cloud explosion results in a shock wave. Damages from a shock wave and the associated overpressure range from serious direct health effects (lung damage, damage to hearing, whole-body displacement phenomena), to serious indirect health effects resulting from fragments and debris from damaged structures, to collapses of buildings and damage of window-panes. Refs. [1,21] provide dose relationships and Probit functions for all these types of consequences. A shock wave may also provoke an accident to a vehicle moving along the highway. Since the consequences of interest in this analysis are fatalities induced to users of the highway, of interest are shock waves that can cause an accident to a vehicle severe enough to cause the death of the passengers. It has been assumed that such severe damages to vehicles are inflicted by shock waves strong enough to cause the collapse of buildings. Consequently the dose and Probit functions considered are these corresponding to this type of damages, given by Refs. [1,21].

For overpressure equal to P_s and impulse I_s, given by $I_s = 1/2\, P_s t_p$, the dose function used is:

$$D(x,y) = \left(\frac{40\,000}{P_s}\right)^{7.4} + \left(\frac{460}{I_s}\right)^{11.3} \tag{17}$$

where

P_s is the overpressure (Pa)
I_s is the impulse of the shock wave (Pa s)
t_p is the positive phase duration of the shock wave (s)

For a flash fire, the intense phenomenon is the intense thermal radiation. As discussed in Section A.2, it has been assumed that any person in a vehicle within the envelope of the flammable cloud is assumed to receive a lethal dose of thermal radiation.

A.4. Individual risk from overpressure

The probability of lethality owing to the shock wave created by a UVCE is given by the following Probit function [21].

$$Y_1 = 5 - 0.22 \ln D(x,y) \tag{18}$$

The probability that an individual at a point (x,y) at the vicinity of the storage facility will die, *provided* that the release category k has occurred, is then calculated as follows: for each point (x,y) around the explosion point the overpressure is calculated according to Eq. (15) and the probability of death, $R_{ex}(x,y)$, according to Eqs. (3) and (18).

A.5. Individual risk from a flash fire

As discussed in Section A.2 for the flash fire phenomenon, we assumed that any one within the trace of the flammable cloud receives a lethal dose of thermal radiation while for any person outside the trace the probability of death is assumed equal to zero.

In mathematical terms, these remarks can be cast in the following way:

$$R_{\mathrm{ff}}(x,y) = \begin{cases} 1 & \text{if } (x,y) \epsilon T_{\mathrm{R}}(t) \\ 0 & \text{otherwise} \end{cases} \tag{19}$$

where $T_{\mathrm{R}}(t)$ is the trace of the flammable cloud at time t.

Finally, the individual risk conditional on the plant damage state #1, that is, release of LPG and dispersion is

$$R_1(x,y) = \frac{2}{3} R_{\mathrm{ex}}(x,y) + \frac{1}{3} R_{\mathrm{ff}}(x,y) \tag{20}$$

since according to Refs. [19,20], given the ignition of an LPG cloud, the relative likelihood of UVCE is $2/3$ vs. $1/3$ for flash fire.

A.6. The LPG BLEVE model

There is only one release category associated with the BLEVE phenomenon and the consequences are calculated as follows.

In the general case of a fire, the intensity of thermal radiation released per unit area as a function of the distance r from the center of the trace of the fire is given by:

$$Q(r) = E \tau_{\alpha} \upsilon_{\mathrm{F}} \tag{21}$$

where

$Q(r)$	intensity of thermal radiation $(\mathrm{kw/m^2})$
E	emissive power per unit area $(\mathrm{kw/m^2})$
τ_{α}	atmospheric transmissibility $\cong 0.7$
υ_{F}	view factor
r	distance from the center of the fireball projection on the ground (m),

In the case of a BLEVE, the view factor υ_{F} and the emissive power E are calculated by the following equations:

$$\upsilon_{\mathrm{F}} = \frac{D^2}{4\left[\gamma^2 D^2 + r^2\right]} \tag{22}$$

$$E = \frac{M H_{\mathrm{c}} f}{\pi D^2 T} \tag{23}$$

where f is a function of pressure in the tank and it is calculated according to:

$$f = 0.27 P^{0.32} \tag{24}$$

The flame radius is given by:

$$D = 6.48\,M^{0.325} \tag{25}$$

The duration of the BLEVE is given by:

$$T = 0.852\,M^{0.26} \tag{26}$$

and

$$r = \left(x^2 + y^2\right)^{1/2} \tag{27}$$

where

r	distance from the center of the fireball projection on the ground (m)
x, y	coordinates of a point with the source at the center (0,0)
D	radius of fireball (m)
γD	height of the center of the fireball from the ground expressed as a fraction of the fireball diameter
f	fraction of heat released due to combustion that is radiated from the Fireball
M	mass of combustion (kg)
T	duration of fireball (s)
H_c	heat of combustion (kJ/kg)
P	pressure in tank (atm)

Exposure of an individual to the thermal radiation might result in injury or death depending on the degree of exposure. A measure of this exposure is the 'dose' of heat that an individual is receiving and it is given by [22–25]

$$D(x,y) = \left[Q(x,y)\right]^{4/3} t \tag{28}$$

where t is exposure time (s)

Refs. [22–25] provide also the Probit function for exposure to thermal radiation as:

$$Y_2 = -14.9 + 2.56 \ln\{D(x,y)\} \tag{29}$$

which in turn yields the probability of death for an individual standing at a distance r from the source for t seconds, according to Eq. (3).

A.7. Jet fire

The intensity of thermal radiation in the jet fire case is again given by Eq. (21) while the average emissive power is calculated by Eqs. (29) and (30) [20] below where it is assumed that the jet is a cylinder. The view factor v_F in Eq. (21) for a cylinder with height equal to the length of the jet and radius equal to that of the orifice is calculated according to Eqs. (46)–(52) in Section A.6 below, again from Ref. [20].

The emissive power is:

$$E = \frac{0.3 \cdot \dot{m}'' H_c}{A} \tag{30}$$

with

$$A = \frac{\pi d_f^2}{2} + \pi d_f L_f \tag{31}$$

$$L_f = \frac{d_u}{K_1} \tag{32}$$

$$d_f = \frac{d_u}{2 K_1 b_2^{1/2}} \tag{33}$$

K_1 and b_2 are calculated from:

$$K_1 = \frac{0.32 \rho'_{g,a}}{\sqrt{\rho'_{g,0}}} \frac{b_1}{b_1 + b_2} j_{st} \tag{34}$$

$$b_1 = 50.0 + 48.2 \rho'_{g,a} - 9.95(\rho'_{g,a})^2 \tag{35}$$

$$b_2 = 23 + 41 \rho'_{g,a} \tag{36}$$

$$j_{st} = \sqrt{J_{UEL} J_{LEL}} \tag{37}$$

and $\rho'_{g,a}$, $\rho'_{g,0}$ from:

$$\rho'_{g,a} = \frac{\rho_g}{\rho_a} \tag{38}$$

$$\rho'_{g,0} = \frac{\rho_{g,0}}{\rho_a} \tag{39}$$

where

A	surface of jet (m^2)
$\dot{m}''$	burning rate (kg/s) equal to outflow rate
H_c	heat of combustion (J/kg)
d_f	diameter of jet (m)
L_f	height of jet (m)
d_u	diameter of orifice (m)
j_{st}	stoichiometric volume fraction
$\rho'_{g,a}$	relative density of gas, to air
$\rho'_{g,0}$	relative density of gas at the orifice, to air
$\rho_{g,0}$	density of gas at the orifice before outflow (kg/m^3)
ρ_g	density of gas, at ambient temperature (kg/m^3)
ρ_a	air density, at ambient temperature (kg/m^3)
J_{UEL}	upper flammability limit
J_{LEL}	lower flammability limit

A.8. Pool fire model

The heat radiation load Q in a pool fire, which is released per unit area in case of a pool fire, is calculated again according to Eq. (21).

The average emissive power E in this case is calculated according to the following equation [20].

$$E = \frac{0.35\dot{m}'' H_c}{72\dot{m}''^{0.61} + 1} \tag{40}$$

The burning rate is calculated for a non boiling substance from Eq. (41) [20] as follows:

$$\dot{m}'' = \frac{10^{-3} H_c}{H_v + c_v \Delta T} \text{ where } \Delta T = T_B - T_{amb} \tag{41}$$

For the calculation of the view factor in Eq. (21) the pool length L is needed, which is calculated according to the following equations [25].

For still air:

$$L = 42D\left[\frac{\dot{m}''}{\rho_0\sqrt{gD}}\right]^{0.61} \tag{42}$$

otherwise,

$$L = 55D\left[\frac{\dot{m}''}{\rho_0\sqrt{gD}}\right]^{0.67} U_*^{0.21} \tag{43}$$

$$U_* = \frac{U}{U_c} \tag{44}$$

$$U_c = \left[\frac{\dot{m}'' gD}{\rho_0}\right]^{1/3} \tag{45}$$

note that, if $U < U_c$, $U_* = 1$, where

T_{amb} ambient temperature (K)
T_B boiling temperature (K)
H_v heat of vaporization (J/kg)
H_c heat of combustion (J/kg)
c_v specific heat (J/kg K)
D pool diameter (m)
U wind speed (m/s)
g gravity acceleration (m/s^2)
ρ_0 density of air (kg/m^3)

The only factors (apart from the physical properties of the material) affecting the intensity of the thermal radiation are the pool diameter D and the ambient temperature T_{amb}. On the other hand, the total mass of oil involved in the phenomenon determines its duration. Since the radius of the dike where the pool is formed is constant and the effect of the ambient temperature minimal, only one release type is defined for this plant damage state.

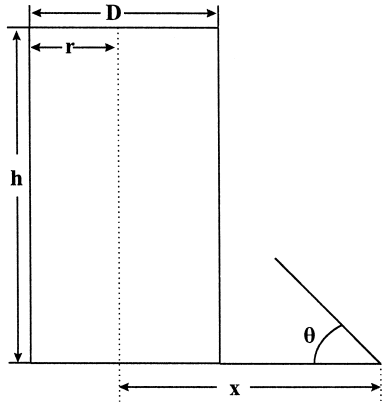

Fig. 12. Schematic representation of view factor in a pool fire.

The consequences of exposure to heat radiation from a jet or a pool fire are the same as those from any other heat source and the corresponding Probit function and probability of death are given by Eqs. (28) and (29). The calculation of the view factor in Eq. (21) is presented in the following section.

A.9. View factor for a vertical cylindrical radiator

The view factor for the cases of a jet fire and a pool fire is calculated according to Eqs. (46)–(52) taken from Ref. [20] for a cylinder with height, the height of the flame and radius, the radius of the orifice (pool), on the vertical plane (see Fig. 12).

By defining:

$$h_r = h/r \tag{46}$$

$$x_r = x/r \tag{47}$$

$$A = (x_r + 1)^2 + h_r^2 \tag{48}$$

$$B = (x_r - 1)^2 + h_r^2 \tag{49}$$

then, for a horizontal plane at ground-level ($\theta = \pi/2$):

$$v_{\mathrm{Fh}} = 1/\pi\left\{\tan^{-1}\sqrt{(x_r+1)(x_r-1)} - \left(x_r^2 - 1 + h_r^2\right)/\sqrt{AB}\,\tan^{-1}\sqrt{(x_r-1)\,A/\left[(x_r+1)\,B\right]}\right. \tag{50}$$

and for a vertical plane at ground-level ($\theta = 0$):

$$v_{\mathrm{Fv}} = 1/\pi\left\{1/x_r\tan^{-1}\left(h_r/\sqrt{\left(x_r^2-1\right)}\right) + h_r(A - 2x_r)/x_r\sqrt{AB}\,\tan^{-1}\sqrt{(x_r-1)\,A/\left[(x_r+1)\,B\right]} - h_r/x_r\tan^{-1}\sqrt{(x_r-1)/(x_r+1)}\right\} \tag{51}$$

The maximum view factor was used in the calculations (as a worst case estimate) and is equal to

$$V_{\mathrm{Fmax}} = \sqrt{\left(v_{\mathrm{Fh}}^2 + v_{\mathrm{Fv}}^2\right)} \tag{52}$$

References

[1] AICHE/CCPS, Guidelines for evaluating the characteristics of vapor cloud explosions, flash fires, and BLEVEs, Center for Chemical Process Safety, American Institute of Chemical Engineers, New York, 1994.

[2] P.A. Davies, A guide to the evaluation of condensed phase explosions, J. Hazardous Mater. 33 (1993) 1–33.

[3] J.C. Leyer, D. Desbordes, J.P. Saint-Cloud, A. Lannoy, Unconfined deflagrative explosion without turbulence: experiment and model, J. Hazard. Mater. 34 (1993) 123–150.

[4] A.C. van den Berg, A. Lannoy, Methods for vapour cloud explosion blast modeling, J. Hazardous Mater. 34 (1993) 151–171.

[5] D. Bjerketvedt, J. Roar Bakke, K. van Wingerden, Gas explosion handbook, J. Hazardous Mater. 52 (1997) 1–150.

[6] H. Montiel, J.A. Vilchez, J. Casal, J. Arnaldos, Mathematical modeling of accidental gas releases, J. Hazardous Mater. 59 (1998) 211–233.

[7] NFPA, 30 Flammable and Combustible Liquid Codes, 1987.

[8] AICHE/CCPS, Guidelines for chemical process quantitative risk analysis, Center for Chemical Process Safety, American Institute of Chemical Engineers, New York, 1989.

[9] Guidelines for Integrated Risk Assessment and Management in Large Industrial Areas, Jointly sponsored by IAEA, UNEP, UNID, WHO, IAEA-TECDOC-XXX, Vienna, 1995.

[10] G. Purdy, Risk analysis of the transportation of dangerous goods by road and rail, J. Hazardous Mater. 33 (1993) 229–259.

[11] I.A. Papazoglou et al., Probabilistic safety analysis in chemical installations, J. Loss Prev. Process Ind. 5 (3) (1992) .

[12] I.A. Papazoglou et al., On the management of severe chemical accidents. DECARA: a computer code for consequence analysis in chemical installations. Case study: ammonia plant, J. Hazardous Mater. 31 (1992) 135–153.

[13] I.A. Papazoglou, O. Aneziris, G. Bonanos, M. Christou, SOCRATES: a computerised toolkit for quantification of the risk from accidental releases of toxic and/or flammable substances, in: A.V. Gheorghe (Ed.), Integrated Regional Health and Environmental Risk Assessment and Safety Management, published in Int. J. Environment and Pollution, Vol. 6, Nos. 4–6, 1996, pp. 500–533.

[14] F.P. Less, Loss prevention in the process industries, Vol. 1, Butterworths, London, 1996.

[15] R.L. Iman, M.J. Shortencarier, A FORTRAN 77 Program for the Generation of Latin Hypercube Random Samples, NUREG/CR-3624, SAND-2365, Sandia National Laboratories, Albuquerque, NM, 1984.

[16] S.F. Jagger, Development of CRUNCH: A dispersion model for continuous releases of a denser-than-air vapour into the atmosphere, UKEA, SRD Report R229, 1983.

[17] L.S. Fryer et al., DENZ: a computer program for the calculation of the dispersion of dense toxic or explosive gases in the atmosphere, UKEA, SRD Report R152, 1979.

[18] G.D. Kaiser, A review of models for predicting the dispersion of ammonia in the atmosphere, plant/operation progress, in: Hawthorne (Ed.), Petroleum liquids, fire and emergency control, Vol. 8, No. 1 (1989), Prentice Hall, NJ, 1987.

[19] LPG, A Study, General Report, TNO, Apeldoorn, 1983.

[20] Methods for Calculation of the Physical Effects of the Escape of Dangerous Materials (Liquids and Gases), Netherlands Organisation for Applied Scientific Report (TNO), 1992.

[21] Methods for the determination of possible damage, CPR 16E, TNO, 1989.

[22] A.F. Roberts, The effect of conditions prior to loss of containment on fireball behaviour, the Assessment of Major Hazards Symposium, IEChem Sym Series No. 71, Manchester, 1982.
[23] K.S. Mudan, Thermal radiation hazards from hydrocarbon fireballs, in: A.D. Little (Ed.), 1982.
[24] J. Moorhouse, Thermal radiation hazards from large pool fires and fireballs—a literature review, The Assessment of Major Hazards IEChem Sym Series No. 71, Manchester, 1982.
[25] W.P. Crocker, D.H. Napier, Thermal radiation hazards of liquid pool fires and tank fires, Hazards in process Industries, IChemE, 1985.